Available online at www.sciencedirect.com

ScienceDirect

Solar Energy 103 (2014) 62–69

SOLAR ENERGY

www.elsevier.com/locate/solener

Corrosion resistance of Hastelloys in molten metal-chloride heat-transfer fluids for concentrating solar power applications

K. Vignarooban [a], P. Pugazhendhi [b], C. Tucker [b], D. Gervasio [b], A.M. Kannan [a,*]

[a] Department of Engineering and Computing Systems, Arizona State University, Mesa, AZ 85212, USA
[b] Department of Chemical and Environmental Engineering, University of Arizona, Tucson, AZ 85721, USA

Received 5 July 2013; received in revised form 29 January 2014; accepted 1 February 2014
Available online 28 February 2014

Communicated by: Associate Editor Ranga Pitchumani

Abstract

Corrosion rates have been estimated for commercial Hastelloys C-276, C-22 and N types in eutectic molten salts containing NaCl, KCl and $ZnCl_2$ using steady-state potentiodynamic method (0.2 mV s^{-1} within ~±30 mV from the open circuit voltage). Hastelloy C-276 exhibited the lowest corrosion rates of ~10 and 40 μm per year in 13.4NaCl–33.7KCl–52.9$ZnCl_2$ (mol%) salt at 250 and 500 °C, respectively. The potentiodynamic method was validated by conducting traditional immersion test for corrosion rate estimation on C-276 Hastelloy in 13.4NaCl–33.7KCl–52.9$ZnCl_2$ (mol%) at 500 °C (corrosion rate ~50 μm per year). Among the samples evaluated, Hastelloy N showed highest corrosion rate of >150 μm per year at 500 °C.

Keywords: Halide eutectic molten salts; High temperature corrosion; Potentiodynamic polarization; Corrosion rate

1. Introduction

The heat transfer fluid used to carry thermal energy from a solar concentrator to a steam generator is a vital component in concentrated solar power systems. The heat transfer fluids currently used in CSP systems (for description of acronyms, see Table 1) are either hydrocarbon oils or alkali-nitrate based eutectic molten salt mixtures (Guillot et al., 2012; Fernandez et al., 2012; Goods and Bradshaw, 2004; Olivares, 2012; Dunn et al., 2012). Using hydrocarbon oils as the HTF require that the chamber for collecting stored heat be flooded with nitrogen in order to prevent fire or explosions. Nitrate salts are less flammable but the quantity required to achieve the International Energy Agency's target of 630 GW of CSP in 2050 would represent 30 times the current mine production of Chile (Guillot et al., 2012). Both materials have a limited operating temperature range. Efficiency increases with increasing temperature difference, so ideal heat transfer fluids would operate beyond 1000 °C, but hydrocarbon oils are limited to 250 °C, and alkali-nitrate based molten salts are thermally stable only up to 600 °C (Dunn et al., 2012).

There is a pressing need to find compatible heat transfer fluids for CSP systems created from inexpensive naturally abundant materials which are stable up to 1300 °C (High temperature, 2012). Such high temperature HTFs can be formed by mixing ionic and covalent halides to form novel low melting (200 °C), high boiling (>1000 °C) eutectics. These new molten-salts have been proposed for improving the efficiency and cost competitiveness of future CSP systems. Ionic chloride salts, including NaCl and KCl are abundant in nature and boil at temperatures higher than 1400 °C. When these are mixed with low melting (200 °C)

* Corresponding author. Tel.: +1 (480) 727 1102; fax: +1 (480) 727 1549.
E-mail address: amk@asu.edu (A.M. Kannan).

http://dx.doi.org/10.1016/j.solener.2014.02.002
0038-092X/

Table 1
Nomenclature of frequently used parameters and their respective acronyms.

Acronym	Definition	Units (if any)
ASTM	American society for testing of Materials	–
CR	Corrosion rate	μm per year
CSP	Concentrating solar power	–
E_{corr}	Corrosion potential	mV
EW	Equivalent weight	–
HTF	Heat transfer fluid	–
i_{corr}	Corrosion current density	μA cm^{-2}
OCV	Open circuit voltage	mV
SCE	Saturated calomel electrode	–

covalent metal halides, such as $ZnCl_2$ and $AlCl_3$, the covalent metal halide is stabilized by chloride complexation to the transition metal. There is a structural mismatch between the components due to the difference in size and shape of the covalent and ionic chlorides which leads to the formation of a low melting and stabilized eutectic mixture. These mixtures have been found to be thermally stable at high temperatures desired for use as heat transfer fluids in CSP systems (Li, 2013).

Higher operating temperatures increase efficiency but also promote faster corrosion of the Hastelloy or stainless steel materials used to make the pipe and vessels that contain these molten-salt mixtures. It is known that chloride salts in aqueous solution can break down the passive oxide layer and promote corrosion reactions with metals (Sorell, 1997). The corrosion mechanism is different in molten-salt systems compared to aqueous ones, but it is reasonable to expect that these chloride species in molten-chloride-salt systems would also break down the passive oxide layer and promote corrosion reactions. Several works on these molten-salt corrosion issues have been performed in the past (Slusser et al., 1985; Ravi Shankar et al., 2012; Trinstancho-Reyes et al., 2011; Abramov et al., 2010; Ni et al., 2011; Ambrosek, 2011; Williams, 2006).

One of the earliest works on corrosion issues of CSP salts was performed in 1985 by Slusser et al. (1985). They studied corrosion behavior of both iron-based and nickel-based alloys in nitrate-nitrite salts between 510 and 705 °C and found that nickel alloys with 15–20% chromium content performed the best at high temperatures. Corrosion of nickel containing alloys in molten LiCl–KCl medium has been studied in a recent work (Ravi Shankar et al., 2012) and it has been reported that Inconel 600 and Inconel 690 alloys showed better corrosion resistance than Inconel 625 and alloy 800H at high temperatures. In another recent work (Trinstancho-Reyes et al., 2011), corrosion behavior of Inconel 718 alloy in molten-salt was investigated by electrochemical impedance spectroscopy. Abramov et al. (2010) have done a spectro-electrochemical study of stainless steel corrosion in NaCl–KCl melt and found out that the major corrosion products of steel are iron, manganese and chromium species. To the best of our knowledge, corrosion behavior of Hastelloys in NaCl–KCl–$ZnCl_2$ ternary molten-salt mixtures has not been reported in the literature.

Corrosion rates can be estimated using immersion (gravimetric weight loss) tests or electrochemical tests. Immersion testing is accurate but takes weeks to months to complete so can only give information about average corrosion rates over this time. Electrochemical testing can be done in minutes, so it offers the advantage of rapid screening to estimate the instantaneous corrosion rate (Wang, 2006). Electrochemical methods such as potentiodynamic polarization, potentio-staircase and cyclic voltammetry are often used for laboratory corrosion testing (Ciubotariu et al., 2008). Among these, the steady state potentiodynamic polarization method is most commonly used to estimate corrosion rates (Hsieh et al., 2010; Zhang et al., 2009; Poursaee, 2010; Wang and Chao, 2012; Zou et al., 2011). In the potentiodynamic polarization method, the metal of interest is a working electrode in an electrolyte representative of the corrosive environment. The working electrode potential is controlled and slowly scanned through a small voltage window (~±30 mV from the OCV) as the resulting current is recorded. From the resulting data, the corrosion current can be estimated at the corrosion potential, and this is used to estimate the corrosion rate.

In the present study, the corrosion rates of commercial nickel based Hastelloy types in NaCl–KCl–$ZnCl_2$ halide eutectic molten-salt mixtures up to 500 °C have been estimated using a steady-state electrochemical potentiodynamic as well as gravimetric methods. Hastelloys C-276 and C-22 show reasonably good corrosion resistance in the molten-salt environments up to 500 °C. In particular, Hastelloy C-276 exhibited an exceptionally low corrosion rate of about 10 and 40 μm per year in NaCl–KCl–$ZnCl_2$ eutectic system at 250 and 500 °C, respectively, through electrochemical method. The corrosion rate values obtained by the electrochemical method at 500 °C were also validated by gravimetric method for the same Hastelloy coupons.

2. Experimental

2.1. Materials

NaCl, KCl and $ZnCl_2$ were purchased from Alfa Aesar for making three different molar compositions of NaCl–KCl–$ZnCl_2$ (Salt #1: 13.4–33.7–52.9, Salt #2: 18.6–21.9–59.5 and Salt #3: 13.8–41.9–44.3) eutectic salt mixtures (Li, 2013; Bale et al., 2009). The salt compositions, Salt #1, #2 and #3 have melting temperatures of 204, 213 and 229 °C, respectively (Bale et al., 2009). All the salts used in this study were stored in inert atmosphere or under vacuum before loading them into the furnace where the salt mixture was heated to above 200 °C within few minutes so there was little bulk water or metal oxides. The only source of oxygen is from molecular oxygen or water diffusing into the salt from air. Silver (99.95%) and silver chloride (99.9%) powders purchased from Strem

Chemicals (Strem Chemicals, Inc., Newburyport, MA, USA) were used for reference electrode. Hastelloy types C-276 (thickness: 0.4 mm), C-22 (thickness: 0.6 mm) and N (thickness: 1.0 mm) procured from Haynes International Inc., Kokomo, IN, USA (Corrosion Resistant Alloys. Haynes International Inc., 2013) were evaluated for their corrosion behavior at two different temperatures of 250 and 500 °C. The major elements in these alloys are Ni, Co, Cr, Mo, W and Fe. Haynes product literature on these alloys provides the specific composition along with trace elements and is given in Table 2 (Corrosion Resistant Alloys. Haynes International Inc., 2013).

2.2. Experimental set-up

A schematic of the experimental set-up for conducting potentiodynamic scans of Hastelloy as the working electrode in molten salt at high temperatures is shown in Fig. 1. The high temperature electrochemical quartz cell fabricated at Technical Glass Products (www.technical-glass.com, Painesville, OH) has provisions to hold the working, counter and reference electrodes into the molten-salt mixture. In order to eliminate any mixed potentials in the three electrode system, the counter electrode material was the same alloy used as the working electrode in every measurement. Ag/AgCl reference electrode was made by filling a homogenous mixture of equal amounts of Ag and AgCl powders in a quartz tube with a quartz frit (pore size ~ 20–30 μm). Electrical contact was established by inserting Ag wire (1 mm diameter) through the quartz tube into the Ag/AgCl mixture. The potential of the reference electrode was calibrated versus a saturated calomel electrode (SCE) in saturated aqueous KCl solution only at room temperature and recorded a potential difference of −60 mV vs SCE. The Ag/AgCl reference electrode was dried before using it at high temperatures. Hence there is no water in the Ag/AgCl reference electrode. As shown in the experimental set-up in Fig. 1, all the corrosion measurements were made with the reference electrode at the operating temperature. The temperature of the electrochemical quartz cell was controlled by inserting it into the hot zone from the top of the programmable muffle furnace.

2.3. Potentiodynamic method

The surface of the as-received Hastelloy samples was cleaned with acetone before conducting the potentiodynamic scans. The geometric area of the working electrode was 2.6 cm^2 and that of counter electrode was 4 cm^2. The potentiodynamic polarization experiments were conducted using a PARSTAT-2273 Advanced Electrochemical System at a scan rate of 0.2 mV s^{-1} starting at −30 mV and ending at +30 mV from the OCV of the working electrode versus the Ag/AgCl reference electrode. The potentiodynamic scans for corrosion rate estimation were conducted in air at 250 and 500 °C. The polarization scans were started after the OCV reached a stable value at every test condition. For every experimental test condition, a new eutectic salt mixture and new Hastelloy electrodes (working and counter electrodes) were used. As shown in Fig. 2a, the corrosion current density values are determined from tangent lines drawn on the anodic and cathodic portions of the current density versus potential curves and intersecting at the corrosion potential, using '*Power Suite*' software in the PARSTAT-2273. The corrosion rates (CR) are estimated by using the formula derived from Faraday's Law, as given by ASTM Standards G59 and G102 (ASTM International, 2003):

$$\text{CR (in μm per year)} = K_1[(i_{corr}EW)/\rho] \quad (1)$$

where $K_1 = 3.27$ in μm g μA^{-1} cm^{-1} yr^{-1}, i_{corr} is the corrosion current density in μA cm^{-2}, EW and ρ are the equivalent weight and density (g cm^{-3}) of the Hastelloy, respectively. The current density is from the apparent (projected) area not real area, that is, no correction is made for the roughness of the surface.

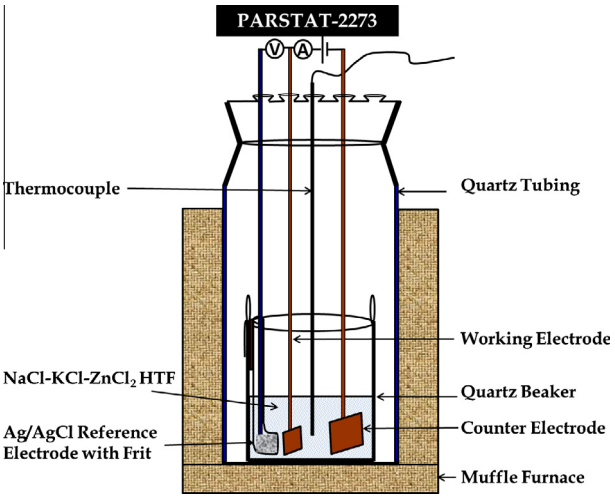

Fig. 1. Schematic of experimental set-up for conducting high temperature corrosion studies by potentiodynamic method for Hastelloys in NaCl–KCl–$ZnCl_2$ eutectic molten salts.

Table 2
Composition of Hatelloy C-276, C-22 and N types.

Hastelloy type	Composition (wt.%)								
	Ni	Co	Cr	Mo	W	Fe	Mn	Si	C
C-276	57	1[a]	16	16	4	5	1[a]	0.08[a]	0.01[a]
C-22	56	2.5[a]	22	13	3	3	0.5[a]	0.08[a]	0.01[a]
N	71	–	7	16	–	5[a]	0.8[a]	1[a]	0.08[a]

[a] Maximum.

2.4. Immersion test

In order to validate the corrosion rate values obtained from the potentiodynamic polarization method, immersion testing was also performed on Hastelloy C-276 in Salt #1. Six different coupons of the C-276 Hastelloy (dimension: 5 cm × 1 cm) were immersed in Salt #1 at 500 °C in six

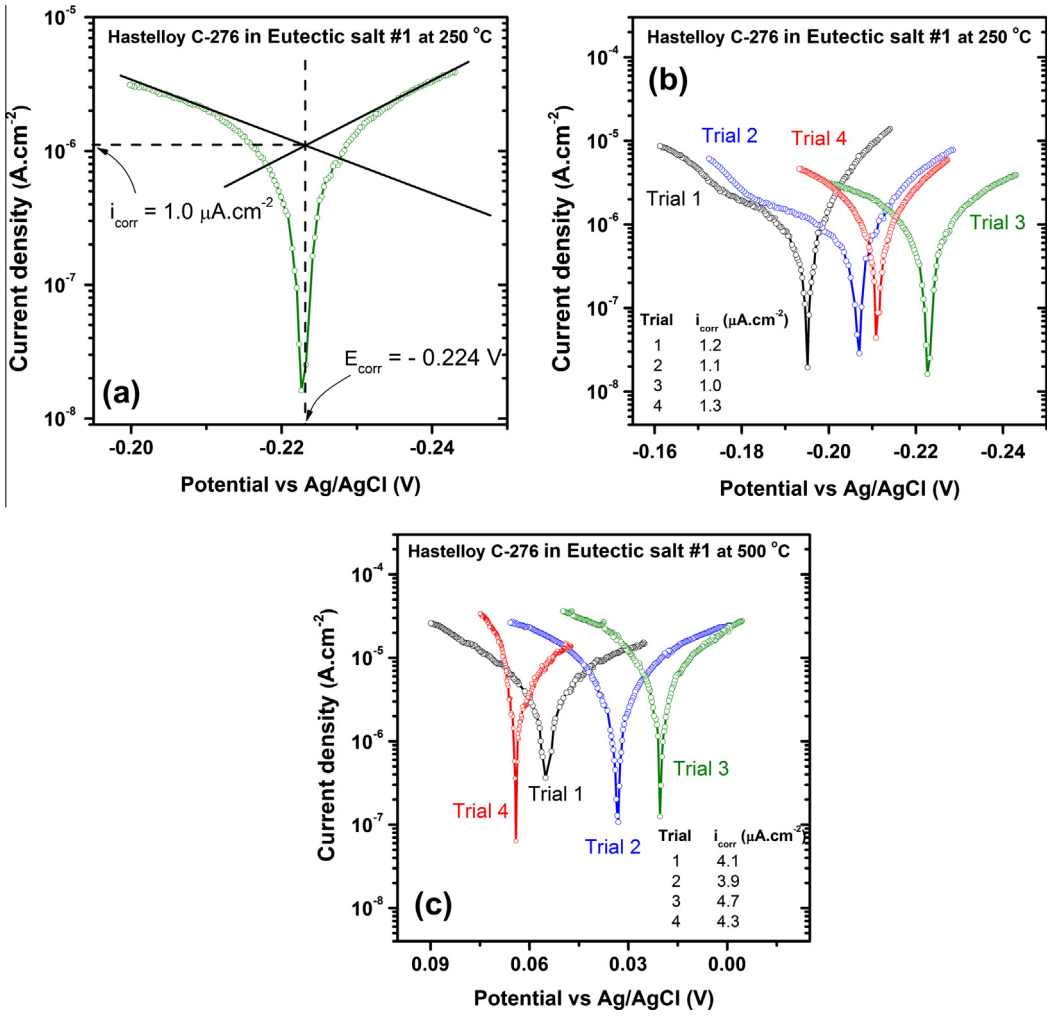

Fig. 2. (a) Potentiodynamic scan at 250 °C for corrosion current and E_{Corr} estimation, (b) and (c) potentiodynamic scans for Hastelloy C-276 in eutectic molten Salt #1 at 250 and 500 °C, respectively for repeatability evaluation.

different quartz test cells and the weight loss was monitored for each coupon every week (sample 1 for 1 week, sample 2 for 2 weeks and so on). The corrosion rate values were calculated using the following equation, assuming uniform dissolution:

$$\text{CR (in μm per year)} = (365)10^4[WL/(\rho AT)] \quad (2)$$

where WL is the weight loss in gram, ρ is density (g cm^{-3}) of the Hastelloy, A is the total immersed area in cm^2, and T is the immersion duration in days.

3. Results and discussion

It is generally accepted that the corrosion rate estimation by using gravimetric weight loss of metals after immersion in corrosive environments provide accurate results for corrosion rates (Wang, 2006; Zou et al., 2011). However, the major drawback of the weight loss method is that it requires several weeks or months in order to get enough weight loss for precise measurements; especially in alloys with low corrosion rates. It is difficult to control corrosion conditions, so the corrosion rate is the average corrosion rate for the average of the corrosion conditions. In this context, the electrochemical corrosion methods are

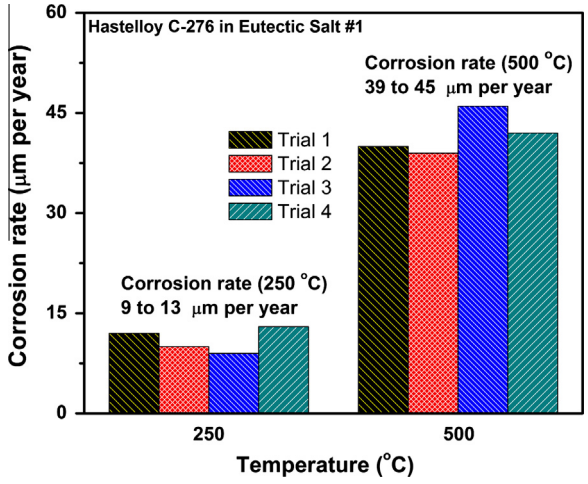

Fig. 3. Histograms showing the repeatability of corrosion rates for Hastelloy C-276 in eutectic molten salt at 250 and 500 °C.

Table 3
Corrosion current density values for different Hastelloy types in NaCl–KCl–$ZnCl_2$ eutectic salt systems.

No.	Hastelloy type	Corrosion current density ($\mu A\ cm^{-2}$)				
		Salt #1: 13.4–33.7–52.9 mol%		Salt #2: 18.6–21.9–59.5 mol%		Salt #3: 13.8–41.9–44.3 mol%
		250 °C	500 °C	250 °C	500 °C	250 °C
1	C-276	1.0	3.8	1.4	4.3	1.9
2	C-22	1.5	4.3	1.8	4.4	2.6
3	N	3.7	16.1	4.8	17.6	4.8

convenient and highly useful as the corrosion rate can be precisely determined in minutes. In addition, electrochemical method also allows one to quickly study the effect of changes in different parameters on the corrosion, such as temperature and pressure under different environments (air, inert environment, and humidity), as well as the temporal evolution of corrosion rate as a function of each or combinations of these effects. The electrochemical method is a rapid measurement method which allows hundreds and hundreds of determinations of metal corrosion rate in the time it takes to do one immersion test.

As described by Hsieh et al. (2010), using a wider polarizing voltage range (e.g., ±250 mV from the OCV) might change the surface properties of the electrode. In order to avoid this problem, the corrosion rates in the present study were obtained by conducting potentiodynamic scans in a narrow voltage range, that is by polarizing the working electrode no more than -±30 mV from the value of the OCV of the working electrode versus the reference electrode. As reported by Zhang et al. (2009), using a very low scan rate such as $0.1 - 0.3\ mV\ s^{-1}$ is an important requirement to ensure the polarization is essentially at steady state and so capacitive effects and the error in the corrosion current is negligible. The repeatability of the corrosion potential (E_{corr}), current density (i_{corr}) and the corresponding corrosion rate was established by taking 4 replicate measurements.

Fig. 2b and c shows the four trials of potentiodynamic polarization scans for the Hastelloy C-276 in Salt #1 at 250 and 500 °C, respectively. The i_{corr} values from the potentiodynamic scans in Fig. 2b and c were estimated following the procedure shown in Fig. 2a. The repeatability of corrosion current density values is seen to be fairly good (ranging from 1 to 1.3 and 3.9 to 4.7 $\mu A\ cm^{-2}$ at 250 and 500 °C, respectively) over the four trials. Even though we used fresh metal piece and fresh salt composition for each and every polarization scans, a small shift in E_{corr} in the range of 10–40 mV has been observed. A similar change in E_{corr} has already been reported in an ASTM standard by performing 33 repeated potentiodynamic polarization scans of the same corrosive system (ASTM International, 2003). The histograms in Fig. 3 consolidate the corresponding corrosion rate values for Hatelloy C-276 in Salt #1 and are 11 ± 1.8 and 42 ± 3 μm per year at 250 and 500 °C.

Similarly, the potentiodynamic scans were conducted for Hastelloys C-276, C-22 and N in three different compositions of Salt #1, #2 and #3 as given in Table 3 both at 250 and 500 °C. As seen in Fig. 4a–f, the potentiodynamic scans are grouped for each Hastelloy type at a particular temperature. Hastelloy samples were not evaluated in Salt #3 at 500 °C as the corrosion rates are relatively higher at 250 °C itself. An important observation in Fig. 4(a–f) is that the corrosion potential follows a pattern. The corrosion potential in Salt #3 < the corrosion potential in Salt #1 and < the corrosion potential in Salt #2 for all 6 sets of different metals and temperatures. A similar pattern can also be seen for the content of $ZnCl_2$ and KCl in these salts, but not for NaCl. The relatively low NaCl content of 13–18% in all the salt mixtures does not appear to have any significant influence. $ZnCl_2$ content in Salt #3 < Salt #1 < Salt #2 and the KCl content in Salt #3 > Salt #1 > Salt #2.

The corrosion rate values were calculated from the corrosion current density results given in Table 3 for the Hastelloy samples in Salt #1, #2 and #3. The corrosion rate values for three Hastelloy types in three different salt compositions are given as 3D histograms in Fig. 5a and b at 250 and 500 °C, respectively. Evidently, the corrosion rates are systematically higher at 500 °C compared to that at 250 °C, inducing higher corrosion rates at higher temperature. It was also observed that the corrosion rates of the Hastelloys; especially, C-276 and C-22 are reasonably low even at 500 °C. These findings are important because using Hastelloy to contain these salts will be useful in terms of corrosion characteristics for heat transfer in CSP applications.

It has been reported that, higher the nickel content in the alloy, then the lower is the corrosion rate, however pure nickel is poorly resistance to corrosion in molten salts (Molten Salt Corrosion, 2007). Consider Hastelloy N studied in this work, it shows higher corrosion rates than Hastelloys C-276 and C-22, even though Hastelloy N has higher nickel content (71% in Table 2) compared to the other two alloys. We believe this higher corrosion of Hastelloy N is mainly due to its low chromium content (7%). It has been reported that chromium is a corrosion resistance material and can be used to form a protective surface layer to safeguard metals from corrosion (Dennis et al., 2013). In one of the earliest molten-salt corrosion work of Slusser et al. (1985), it has been reported using traditional weight loss studies that, 15–20% chromium containing nickel alloys perform as the best corrosive resistance alloys in molten nitrate–nitrite salts at high temperatures, whereas iron alloys perform poorly even with substantial Cr content. There are a couple of other reports in the literature which state that the nickel based alloys with Cr content around 20% performs well in molten-salt corrosive environments (Sorell, 1997; Michel et al., 2011).

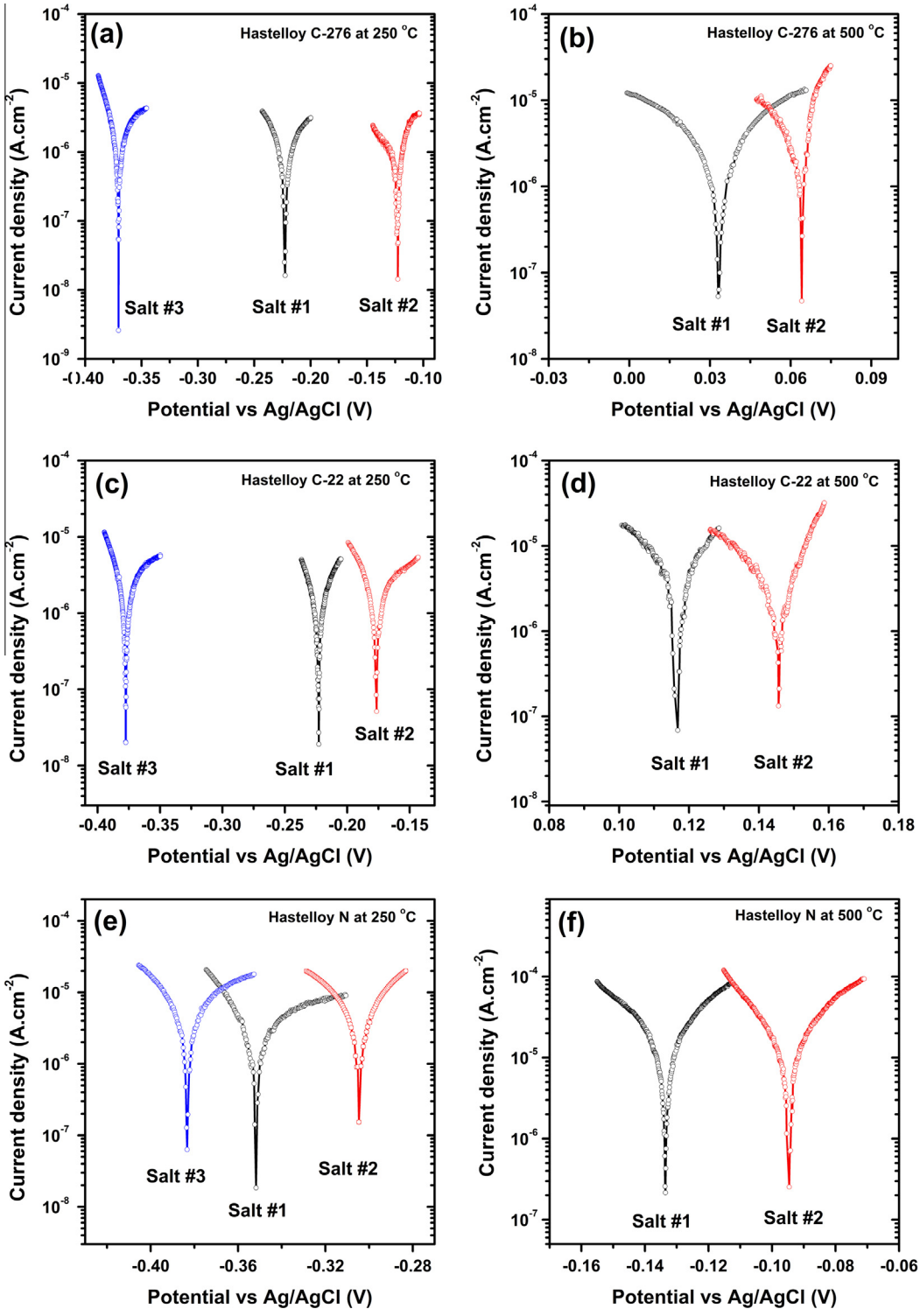

Fig. 4. Potentiodynamic data (a)–(f) for Hastelloy C-276, C-22 and N in Salt #1, #2 and #3 at 250 and 500 °C.

Obviously alloys C-276 and C-22 have Cr content close to 20%, but the Hastelloy N has only 7%. Based on the observed corrosion rates trend, it is surmised that the Hastelloy N is more susceptible for increased corrosion, because Hastelloy N has lower Cr content (7%) compared to C-276 and C-22 alloys (16% and 22% Cr, respectively). It is also worth noting that there are reports that silicon containing alloys, such as RA-330 and Nicrofer-3718 have poor corrosion resistance in the molten salts (Slusser et al., 1985; Molten Salt Corrosion, 2007) and the Hastelloy N contains almost ten times the amount of silicon compared to that in C-276 and C-22.

As shown in Fig. 6, the corrosion rate values calculated from the weight loss method for Hastelloy C-276 at 500 °C

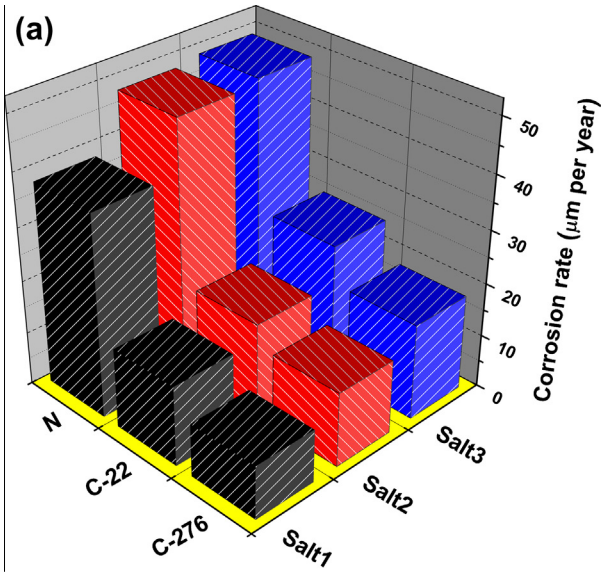

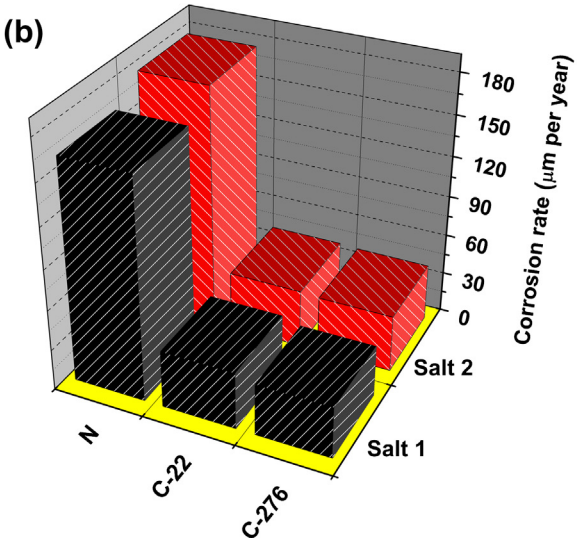

Fig. 5. 3D histograms of corrosion rates for Hastelloys C-276, C-22 and N in NaCl–KCl–$ZnCl_2$ at (a) 250 and (b) 500 °C.

stabilized at about 50 μm per year after 4 weeks of immersion. The corrosion rate values from the 4–6 weeks immersion testing is very close to that obtained by the potentiodynamic polarization scans, validating the results of electrochemical method.

4. Conclusions

In order to establish the corrosion properties of the commonly used piping and container materials in the CSP applications, commercial Hastelloy types C-276, C-22 and N were selected and evaluated in a simulated condition by electrochemical three electrode system in eutectic molten salts comprising NaCl, KCl and $ZnCl_2$ at 250 and 500 °C. Repeatability of the steady-state potentiodynamic polarization scans was established with four trails and the corrosion rates have been estimated for Hastelloys C-276 in 13.4NaCl–33.7KCl–52.9$ZnCl_2$ (mol%) eutectic system

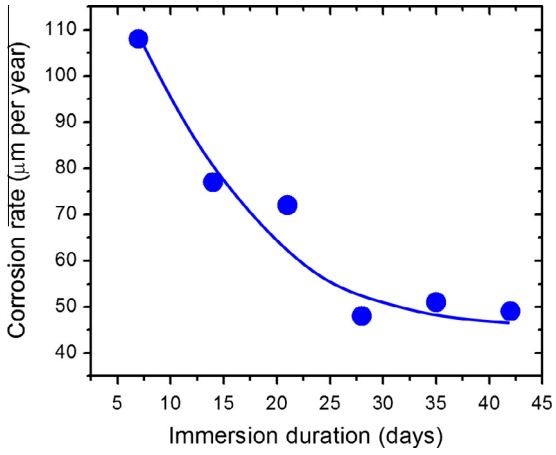

Fig. 6. Corrosion rate values obtained from the immersion test for Hastelloy C-276 (six different coupons) in Salt # 1 at 500 °C for different durations.

before proceeding with other Hastelloy C-22 and N types in other eutectic molten metal chloride salts. Among the Hastelloys evaluated, the type N showed a higher corrosion rate of >150 μm per year at 500 °C and the Hastelloy C-276 exhibited the lowest corrosion rate of ~10 μm per year at 250 °C in 13.4NaCl–33.7KCl–52.9$ZnCl_2$ (mol%) eutectic system. Both the Hastelloy C-276 and C-22 types showed relatively lower corrosion rates in the eutectic systems of Salt #1, #2 and #3. The corrosion rate values obtained from the traditional immersion method for Hastelloy C-276 in 13.4NaCl–33.7KCl–52.9$ZnCl_2$ (mol%) eutectic system also validates the electrochemical method.

Acknowledgements

The Authors would like to thank DOE MURI Grant (Award # DE-EE0005942) for the financial support. Also the authors thank Prof. Pierre Lucas and Prof. Peiwen Li for providing materials and useful discussion.

References

Abramov, A.V., Polovov, I.B., Volkovich, V.A., Rebrin, O.I., Griffiths, T.R., May, I., Kinoshita, H., 2010. Spectroelectrochemical study of stainless steel corrosion in NaCl–KCl melt. ECS Trans. 33 (7), 277–285.

Ambrosek, JW., 2011. Molten chloride salts for heat transfer in nuclear systems. PhD Dissertation in Nuclear Engineering and Engineering Physics, University of Wisconsin-Madison.

ASTM International, vol. 03.02, Standards G 5, G 48, G 59, G 61 and G 102 (ASTM International, 2003: West Conshohocken, PA).

Bale, C.W., Belisle, E., Chartrand, P., Decterov, S.A., Eriksson, G., Hack, K., Jung, I.H., Hang, Y.B., Melancon, J., Pelton, A.D., Robelin, C., Petersen, S., 2009. Fact sage thermochemical software and databases – recent developments. CALPHAD: Comput. Coupling Phase Diagrams Thermochem. 33, 295–311.

Ciubotariu, A.C., Benea, L., Varsanyi, M.L., Dragan, V., 2008. Electrochemical impedance spectroscopy and corrosion behavior of Al_2O_3–Ni nano composite coatings. Electrochim. Acta 53, 4557–4563.

Corrosion Resistant Alloys. Haynes International Inc., Retrieved on June 29, 2013 from <http://www.haynesintl.com/CRAlloys.htm>.

Dennis, R.V., Viyannalage, L.T., Gaikwad, A.V., Rout, T.K., Banerjee, S., 2013. Graphene nano-composite coatings for protecting low-alloy steels from corrosion. Am. Cer. Soc. Bull. 92, 18–24.

Dunn, R.I., Hearps, P.J., Wright, M.N., 2012. Molten-salt power towers: Newly commercial concentrating solar storage. Proc. IEEE 100 (2), 504–515.

Fernandez, A.G., Lasanta, M.I., Ferez, F.J., 2012. Molten salt corrosion of stainless steels and low-Cr steel in CSP plants. Oxid. Met. 78, 329–348.

Goods, S.H., Bradshaw, R.W., 2004. Corrosion of stainless steels and carbon steel by molten mixtures of commercial nitrate salts. J. Mater. Eng. Perform. 13, 78–87.

Guillot, S., Faik, A., Rakhmatullin, A., Lambert, J., Veron, E., Echegut, P., Bessada, C., Calvet, N., Py, X., 2012. Corrosion effects between molten salts and thermal storage material for concentrated solar power plants. Appl. Energy 94, 174–181.

High operating temperature fluids funding opportunity announcement, # DE-FOA-0000567: Multidisciplinary University Research Initiative (MURI) of the US Department of Energy, 2012.

Hsieh, M.K., Dzombak, D.A., Vidie, R.D., 2010. Bridging gravimetric and electrochemical approaches to determine the corrosion rate of metals and metal alloys in cooling systems: bench scale evaluation method. Ind. Eng. Chem. Res. 49, 9117–9123.

Li, PW., Chan, CL., Hao, Q., Deymier, PA., Muralidharan, K., Gervasio, DF., Momayez, M., Jeter, S., Teja, AS., Kannan, AM., 2013. Halide and oxy-halide eutectic systems for high performance high temperature heat transfer fluids. SunShot Concentrating Solar Power Program Review. April 2013, pp. 85–86. <http://www.nrel.gov/docs/fy13osti/58484.pdf>, (accessed 13.11.13).

Michel, G., Berthod, P., Mathieu, S., Vilasi, M., Steinmetz, P., 2011. Chromium deposition on cobalt-based alloys by pack-cementation and behavior of the coated alloys in high temperature oxidation. Open Corros. J. 4, 27–33.

Molten Salt Corrosion. High-Temperature Corrosion and Materials Applications. George Y. Lai, (Ed.). 2007 pp. 409–421 (Chapter 15).

Ni, C.S., Lu, L.Y., Zeng, C.L., Niu, Y., 2011. Electrochemical impedance studies of the initial-stage corrosion of 310S stainless steel beneath thin film of molten $(0.62Li,0.38K)_2$ CO_3 at 650 °C. Corros. Sci. 53, 1018–1024.

Olivares, R.I., 2012. The thermal stability of molten nitrite/nitrates salt for solar thermal energy storage in different atmospheres. Sol. Energy 86, 2576–2583.

Poursaee, A., 2010. Potentiostatic transient technique, a simple approach to estimate the corrosion current density and Stern–Geary constant of reinforcing steel in concrete. Cem. Concr. Res. 40, 1451–1458.

Ravi Shankar, A., Kanagasundar, A., Kamachi Mudali, U., 2012. Corrosion of nickel-containing alloys in molten LiCl–KCl medium. Corros. Sci. Sect. NACE Int. 69, 48–57.

Slusser, J.W., Titcomb, J.B., Heffelfinger, M.T., dunbobbin, B.R., 1985. Corrosion in molten nitrate–nitrite salts. J. Met., 24–25.

Sorell, G., 1997. The role of chlorine in high temperature corrosion in waste-to-energy plants. Mater. High Temp. 14, 137–150.

Trinstancho-Reyes, J.L., Sanchez-Carrillo, M., Sandoval-Jabalera, R., Orozco-Carmona, V.M., Almeraya-Calderon, F., Chacon-Nava, J.G., Gonzalez-Rodriguez, J.G., Martinez-Villafane, A., 2011. Electrochemical impedance spectroscopy investigation of alloy Inconel-718 in molten salts at high temperature. Int. J. Electrochem. Sci. 6, 419–431.

Wang, LL., Martin, SI., Rebak, RB., 2006. Methods to calculate corrosion rates for alloy 22 from polarization resistance experiments. In: Proceedings of ASME Pressure Vessels and Piping Division Conference. July 23–27, 2006, Vancouver, BC, Canada.

Wang, L., Chao, Y., 2012. Corrosion behavior of $Fe_{41}Co_7Cr_{15}Mo_{14}C_{15}$-$B_6Y_2$ bulk metallic glass in NaCl solution. Mater. Lett. 69, 76–78.

Williams, D.F., 2006. Assessment of Candidate Molten Salt Coolants for the NGNP/NHI Heat-Transfer Loop. Oak Ridge National Laboratory.

Zhang, X.L., Jiang, Z.H., Yao, Z.P., Wu, Z.D., 2009. Effects of scan rate on the potentiodynamic polarization curve obtained to determine the Tafel slopes and corrosion current density. Corros. Sci. 51, 581–587.

Zou, Y., Wang, J., Zheng, Y.Y., 2011. Electrochemical techniques for determining corrosion rate of rusted steel in seawater. Corros. Sci. 53, 208–216.